Available online at www.sciencedirect.com
ScienceDirect
Insect Biochemistry and Molecular Biology 37 (2007) 1241–1248
Insect Biochemistry and Molecular Biology
www.elsevier.com/locate/ibmb

Molecular characterization of an inhibitor of apoptosis in the Egyptian armyworm, *Spodoptera littoralis*, and midgut cell death during metamorphosis

Lluïsa Vilaplana, Nuria Pascual, Nathalia Perera, Xavier Bellés*

Department of Physiology and Molecular Biodiversity, Institut de Biologia Molecular de Barcelona (CSIC), Jordi Girona, 18-26, 08034 Barcelona, Spain

Received 22 May 2007; received in revised form 19 July 2007; accepted 23 July 2007

Abstract

The cDNA corresponding to an inhibitor of apoptosis (IAP) from the Egyptian armyworm, *Spodoptera littoralis*, was cloned by RT-PCR. Sequence analysis showed that the IAP of *S. littoralis* (SlIAP) contains two baculoviral IAP repeat (BIR) motifs, followed by a RING finger, an organization which is very similar to that of other lepidopteran IAPs. SlIAP mRNA was detected in ovary, testis, salivary gland, fat body, epidermis, brain and midgut of *S. littoralis*. During the last larval instar, prepupal and pupal stages, brain mRNA levels remained approximately constant, whereas those of midgut showed a large peak centred in the prepupal stage. Midgut morphology changed during metamorphosis from a semi-transparent, cylindrical structure in last instar larvae to a brownish globular mass in pupae. TUNEL assays, LysoTracker staining and caspase-3 immunohistochemistry, indicated that programmed cell death in midgut starts actively at the onset of pupation process, coinciding with the dramatic decrease of SlIAP mRNA levels observed at the same time.

Keywords: Inhibitor of apoptosis (IAP), Midgut cell death, *Spodoptera littoralis*, TUNEL, Caspase, Apoptosis, Autophagy

1. Introduction

Programmed cell death plays an important role in the development and homeostasis of metazoans, and it is also critical in insect embryogenesis and metamorphosis (Vaux and Korsmeyer, 1999). Cells dying by this mechanism show distinct morphological changes including cell shrinkage, membrane blebbing, DNA fragmentation and apoptotic body formation (Wyllie et al., 1980). Programmed cell death is precisely controlled, and regulatory mechanisms have been conserved across animal species during evolution (Fraser and Evan, 1996).

Inhibitor of apoptosis proteins (IAPs) are key regulators of cell death. The first IAPs were discovered in baculoviruses thanks to their capacity to functionally replace the baculoviral p35 protein, another viral apoptosis inhibitor (Crook et al., 1993; Birnbaum et al., 1994). Baculovirus IAPs impair the apoptotic response of the host and extend their survival, thus optimizing viral replication in it. Specifically, IAPs inhibit the caspases that promote cell death (Kumar and Cakouros, 2004), apparently interacting with a particular subset of caspases (Deveraux et al., 1997; Roy et al., 1997; Chai et al., 2003; Zachariou et al., 2003). IAPs have been reported in all eukaryotic groups, including humans (Clem and Duckett, 1998; Deveraux, 1998), and available sequences share a number of structural motifs. Structurally, IAPs are recognized by the presence of 1–3 copies of a motif called baculovirus IAP repeat (BIR) at the amino-terminus (Salvesen and Duckett, 2002). The BIR motif usually comprises approximately 70 amino acids and contains a highly conserved arrangement of Cys/His residues which forms a stable fold that can chelate zinc (Hinds et al., 1999; Sun et al., 1999). BIR motifs are essential for the anti-apoptotic function of IAPs (Vucic et al., 1998), and in the fruitfly *Drosophila melanogaster* they can bind apoptotic inducers, like Grim, Reaper and Hid proteins (Vucic et al., 1997; Vucic et al., 1998;

*Corresponding author.
E-mail address: xbragr@cid.csic.es (X. Bellés).

0965-1748/$ - see front matter © 2007 Elsevier Ltd. All rights reserved.
doi:10.1016/j.ibmb.2007.07.013

Goyal et al., 2000; Yin and Thummel, 2004). In addition to BIR motifs, some IAPs contain a RING finger near the carboxy-terminus, which is also present in other cell proteins (Freemont et al., 1991), although its relevance in the context of cell death depends on the IAP or on the nature of the apoptotic stimulus (Clem and Miller, 1994; Hay et al., 1995). IAPs have been described in a number of lepidopteran species, like *Spodoptera frugiperda* (Huang et al., 2000), *Bombyx mori* (Huang et al., 2001), *Trichoplusia ni* (Liao et al., 2002), *Spodoptera exigua* (GenBank Accession number DQ206460) and *Spodoptera* (= *Prodenia*) *litura* (GenBank Accession number AY751528). A number of organisms have more than one IAP, for example mammals have eight (Liston et al., 2003) and *D. melanogaster* two (Hay, 2000).

In holometabolous insects, programmed cell death removes obsolete larval tissues during larval–pupal transition, and a fine-tuned balance between pro-death factors and anti-death factors regulates the whole death process (Yin and Thummel, 2004). Caspases are typical pro-death factors, whereas IAPs, which directly interact with caspases, are effective anti-death factors. In lepidopterans, in addition to the IAPs mentioned above, two effector caspases have been reported: caspase-1 (Liu et al., 2005; Liu and Chejanovsky, 2006) and another protease called ICE (GenBank Accession Number AY885228).

During insect metamorphosis, midgut tissue undergoes extensive remodelling, and this is especially important in those species where feeding habits change dramatically in the adult. For this reason, midgut remodelling during metamorphosis has been chosen as preferential model to study cell death (Jiang et al., 1997; Lee et al., 2002a; Uwo et al., 2002; Parthasarathy and Palli, 2007). In the present paper, we report the cDNA cloning and characterization of an IAP from the Egyptian armyworm, *Spodoptera littoralis* (SlIAP). Molecular characterization allowed studying *SlIAP* gene expression in brain and gut tissues, which helped to understand the molecular basis of midgut remodelling during metamorphosis. In order to describe this remodelling in detail, we monitored the changes occurring in midgut structure by using TUNEL assays, LysoTracker staining and caspase-3 immunohistochemistry.

2. Material and methods

2.1. Insect rearing and treatments

A colony of *S. littoralis* (Boisduval) (Lepidoptera, Noctuidae), was reared in the laboratory on artificial diet (Poitout and Bues, 1974). Just after egg hatching, larvae were placed in groups of 40–50 into 20×30 cm plastic boxes and maintained in a climatic chamber on a 16 h light: 8 h dark regime, at 25 ± 1 °C and 60–70% relative humidity. Freshly ecdysed last instar larvae (L6) were separated and staged every 24 h and used for experiments. At the end of this instar, prepupal stage (PP) starts. PP stage is characterized by a shortening of the body and suppression of abdominal segments. Pupae were staged as white, freshly formed pupa (P0) and at intervals of 24 h after this moment (P1, P2, P3…). Adults were fed with 20% sugar solution in water. Last larval instar (L6) lasts 4 days, prepupal stage lasts 2 days (PP1, PP2) and pupae lasts 11 days (P0–P11).

2.2. Cloning of SlIAP cDNA

An initial PCR was carried out using a degenerate primer set (LepIAP-F3: TGGGTNGARGGNGAYGAYCC, LepIAP-R1: ATAYCDCACAAGCYTCAGAMA) designed on the basis of conserved BIR and RING sequences of known lepidopteran IAPs. As a template we used 3′ cDNA (Gibco, BRL RACE Kit) obtained from total RNA from young pupae of *S. littoralis*. This yielded a fragment of approximately 460 bp, which was cloned and sequenced. Based on this fragment, specific primers were designed for 5′- and 3′-rapid amplification of cDNA ends (RACE) (Gibco, BRL kits). Following this approach, we completed the cDNA of the SlIAP according to previously described methods (Frohman et al., 1988). To make sure that all amplifications obtained with RACE corresponded to the same molecule, the entire cDNA was amplified with a forward primer designed at the 5′ end and a reverse primer designed at the 3′ end just before the Poly (A)+ tail. PCR products were subjected to electrophoresis on 1.2% agarose gel and subcloned in pSTBlue-1 Acceptor vector (Novagen). Sequencing was carried out by the dideoxynucleotide chain termination method. Clones were sequenced on both strands using SP6 and T7 sequencing primers and internal, specific primers, in an automated fluorescence sequencing system ABI (Perkin Elmer).

2.3. RT-PCR and Southern Blot analyses

Total RNA from tissues under study was isolated using the GenElute Mammalian Total RNA kit (Sigma). An amount between 0.5 and 1 μg of each RNA preparation was used for cDNA synthesis, as previously described (Zhu et al., 2000). For mRNA detection, cDNA samples were subjected to PCR amplification with a number of cycles within the linear range of amplification, being in all cases between 28 and 33 cycles. The primer pair, forward LepIAP-F1: CATCGGAAGCAGAACGTGATGT, and reverse LepIAP-R2: TGCATTCTGAAACGTCCTGCG, were used to amplify a 224 bp fragment of the SlIAP. As a reference, cDNA corresponding to β-actin RNA of *S. littoralis* (GenBank Accession number: Z46873, unpublished) using forward: 5′-GTGATGGTTGGTATGGGTCAGAA-3′, and reverse: 5′-GATCTGGGTCATCTTCTCCCTGT-3′, was amplified in parallel for each cDNA sample. cDNA probes for Southern Blot analyses were generated by PCR with the same primer pairs using plasmid DNAs containing the corresponding cDNA clones as templates. The probes were labelled with fluorescein, using the Gene Images random prime-labelling module

(Amersham Biosciences). RT-PCR followed by Southern blotting of total RNA without reverse transcription did not result in amplification, thus indicating that there was no genomic contamination.

2.4. TUNEL assay

Larval and pupal midguts from *S. littoralis* were dissected out of the developing adult gut under Ringer's saline. They were cut longitudinally and cleaned from their content in such a way that the epithelium which is in contact with the lumen was exposed to the treatment. TUNEL assays were carried out using the in situ Cell Death Detection Kit, Fluorescein (Roche), essentially as described by the manufacturer. Dissected and cut midguts were fixed for 30 min at room temperature in 4% paraformaldehyde in PBS, washed in PT (0.1% Triton-PBS), and permeabilized by incubation in PT-SC (0.1% sodium citrate-0.1% PT) at room temperature for 30 min. Samples were then rinsed in PBS and incubated in TUNEL reaction mixture for 1 h at 37 °C. Finally they were mounted in Mowiol 4-88 (Calbiochem). Sections were examined under a Leica TCS-SP laser scanning confocal microscope and documented using Leica TCS software.

2.5. LysoTracker staining

Midguts from larvae at appropriate stages were dissected in Ringer's saline, and cut as above. First, they were permeabilized during 45 min in PT and then stained with 1 mM of the nuclear dye TOPRO-3 for 10 min (far-red DNA dye excitable with a helium–neon laser; from Molecular Probes, Eugene, OR, USA) diluted 1:500 in PT. After two washes with PBS, samples were stained with LysoTracker Red DND-99 (Molecular Probes), which labels acidic organelles, such as lysosomes, diluted 1:1000 in PBS for 5 min. Finally they were washed twice in PBS for 10 min, mounted in Mowiol 4-88, and examined by confocal microscopy, as above.

2.6. Caspase-3 immunohistochemistry

To detect caspase activity by immunohistochemistry, we used mammalian caspase-3 antibody (Cleaved caspase-3 (Asp 175) antibody from Cell Signalling Technology), which has been shown to reveal caspase homologues in insects, for example in the lepidopteran *Heliothis virescens* (Parthasarathy and Palli, 2007). Tissues were dissected in Ringer's saline and fixed for 30 min with PEM-FA (PEM: 100 mM PIPES, 2 mM EGTA, 1 M $MgSO_4$; PEM-10% formaldehyde (FA) 37%), and they were then washed in PBS 0.2% Tween-20. After three washes of 10 min each, samples were blocked with PBT-NGS (5% normal goat serum, NGS, diluted in 0.1% BSA-0.1% PT) for 1 h at room temperature. Samples were then incubated with caspase-3 antibody at 1:50 diluted in PBT-NGS for 12 h at 4° C. After three washes with PT of 20 min each, samples were incubated with Alexa Fluor 488-Anti-Rabbit IgG (Molecular Probes). Nuclear staining was carried out with 1 mM TOPRO-3, and tissues were mounted as described above. The specificity of signals was checked by including controls without primary antibody treatment. The sections were examined by confocal microscopy, as above.

3. Results

3.1. Structure of Spodoptera littoralis IAP

The complete cDNA of SlIAP is 382 amino acids long (Fig. 1A). It contains a putative start codon preceded by an in-frame stop codon, and a final stop codon followed by a poly(A)$^+$ tail, which indicates that the sequence corresponds to a full-length ORF (GenBank Accession Number: AM709785). SlIAP sequence analysis reveals the presence of two BIR motifs and one RING finger (Fig. 1B). The first BIR motif extends between amino acids 104 and 171 and the second one has the same size but extending between amino acids 214 and 282. Both BIR motifs exhibit the typical distribution of cysteine and histidine residues: $CX_2CX_6WX_9HX_6C$. They are followed by a RING finger domain which is 37 amino acids long and bears the characteristic C3HC4 motif from Cys^{334} to Cys^{371}.

Considering the BIR and RING regions (Fig. 1C–E), SlIAP shows 96% amino acid identity with SeIAP (from *S. exigua*), 93% identity with SfIAP (from *S. frugiperda*) and 83% and 67% identity with TnIAP (from *T. ni*) and BmIAP (from *B. mori*), respectively. The specific IAP of *S. littoralis* nucleopolihedrovirus (SlNPV-IAP) has been described by Liu et al. (2003) as a 15 kDa polypeptide with only one BIR motif, a RING finger and a third specific acidic-rich motif. The alignment of SlIAP and its viral counterpart, SlNPV-IAP, plus other BIR motifs from baculovirus IAPs (data not shown) indicates that the unique viral BIR motif is more similar to the BIR1 than to the BIR2 motif of *S. littoralis*. Pairwise sequence analysis (Fig. 2) of lepidopteran and baculoviral IAP sequences revealed that they show a 22% amino acid identity when comparing SlIAP BIR1 motif with the only SlNPV-IAP BIR motif and 54% within their RING finger. Regarding other baculoviral IAPs, SlIAP show 72% identity with CpGV-IAP (*Cydia pomonella* granulovirus: Crook et al., 1993) and 65% identity with OpNPV-IAP (*Orgyia pseudotsugata* nucleopolihedrovirus: Birnbaum et al., 1994).

3.2. Expression levels of SlIAP gene in brain and midgut

In order to study the tissue distribution of SlIAP expression, we carried out a RT–PCR screening for SlIAP mRNA using as a template total mRNA from ovary, testis, salivary gland, fat body, epidermis, brain and midgut tissues obtained from 4-day-old last larval instar. Results (Fig. 3A) indicated that SlIAP is expressed in all

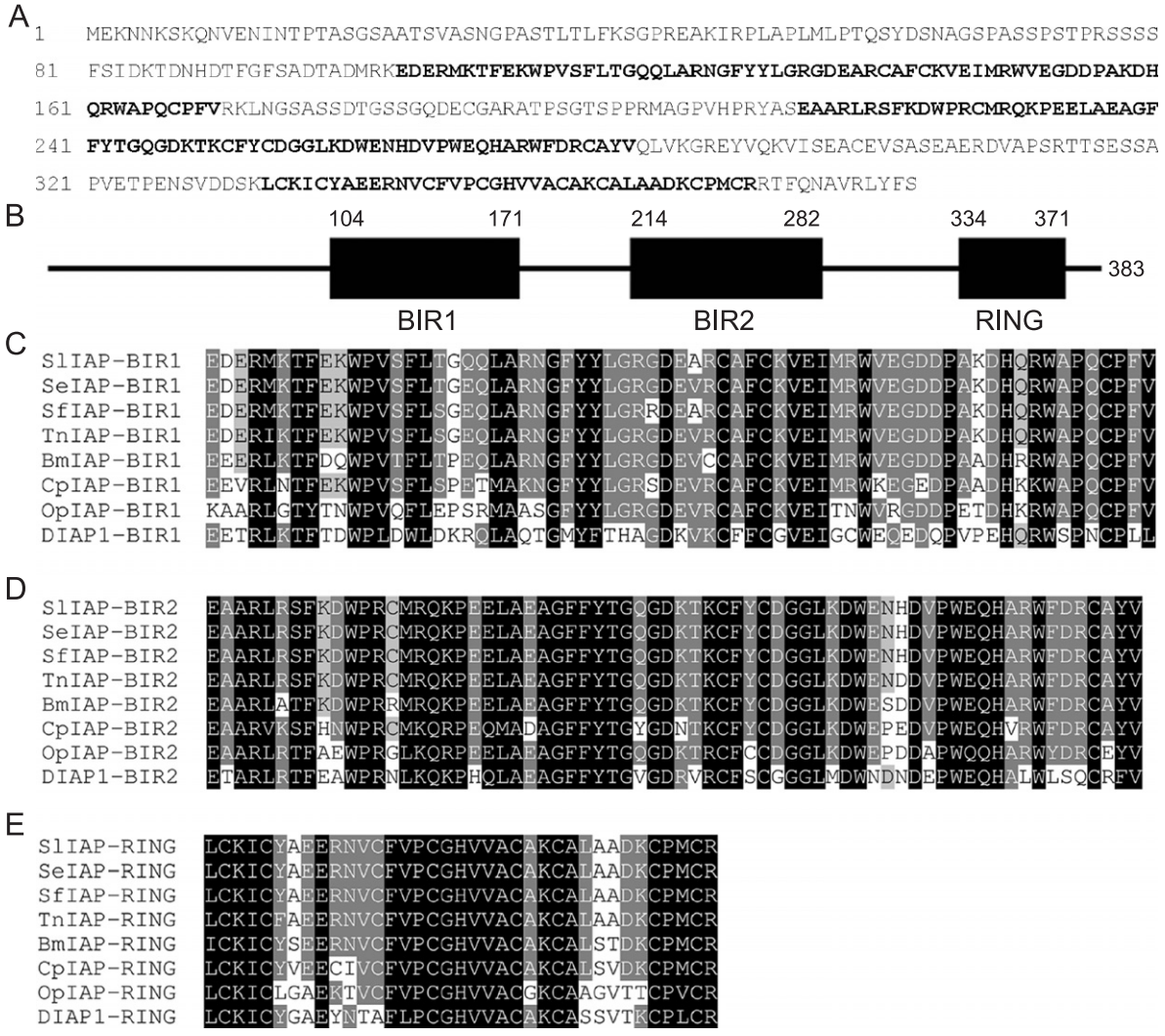

Fig. 1. Structure and organization of *Spodoptera littoralis* IAP (SlIAP). (A) Predicted amino acid sequence. The different characteristic motifs are shown in bold. (B) Organization of BIR motifs and RING finger. (C–E) Alignment of the BIR1 (C), BIR2 (D) and RING (E) regions of SlIAP with the homologous regions of other IAPs. The Genbank accession numbers of sequences used for the alignments are: *Spodoptera exempta* IAP (SeIAP) DQ206460, *Spodoptera frugiperda* IAP (SfIAP) AF186378, *Trichoplusia ni* IAP (TnIAP): AF195528, *Bombyx mori* IAP (BmIAP): AF281073, *Cydia pomonella* granulovirus IAP (CpIAP): P41436, *Orgyia pseudotsugata* IAP (OpIAP): P41437 and *Drosophila melanogaster* IAP (DmIAP): Q24306.

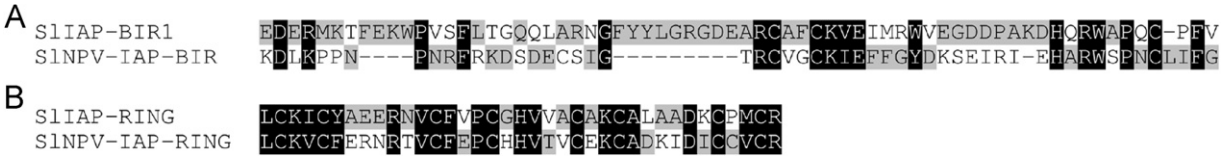

Fig. 2. Comparison of *Spodoptera littoralis* IAP (SlIAP) with *S. littoralis* nucleopolihedrovirus IAP (SlNPV-IAP). (A) Alignment of the amino acid sequence of BIR1 motif and (B) Alignment of the amino acid sequence of RING finger.

tissues analysed. Although the approach followed is not quantitative, results suggest that salivary gland and fat body have much lower relative mRNA levels in comparison with the other tissues examined (Fig. 3A).

Subsequently, we studied the mRNA expression pattern in brain and midgut tissues during the last larval instar, prepupae and pupae. As stated above, larval midgut is completely remodelled during the larval–pupal moult, whereas the brain may serve as a reference, given that neuron generation is continuous from larvae to pupae, and there is no evidence of massive cell death in the stages under study. Results show that SlIAP mRNA levels remain approximately constant in brain tissues (Fig. 3B), whereas in the midgut they rise on days 3 and 4 of last larval instar, show a peak on PP1, start to decrease on PP2, and become dramatically reduced on P0 (Fig. 3C).

3.3. Midgut cell death

Changes observed on midgut SlIAP mRNA levels led us to characterize the process of cell death in this tissue, focusing on its timing from last instar larvae to pupae. Macroscopical examination indicated that larval midgut morphology of *S. littoralis* changes dramatically through the larval–pupal transition (Fig. 4). During the last larval instar, midgut became gradually pigmented from an initial colourless appearance (L1, Fig. 4) to a yellow aspect, which turned to reddish in prepupae (PP2, Fig. 4). The tubular larval midgut increased in size until the end of the larval stage (L4, Fig. 4). Just before entering the prepupal stage, the insect stops feeding, and thereafter the gut shortened due to gut purge. Midgut of freshly formed pupae (P0, Fig. 4) is similar in size to that of prepupae (P0, Fig. 4), but during the pupal stage, it progressively shortens and changes to a globular form (P4, Fig. 4), becoming wider in the anterior part (P7, Fig. 4). Finally, the remnants of larval gut are excreted as the meconium at adult emergence.

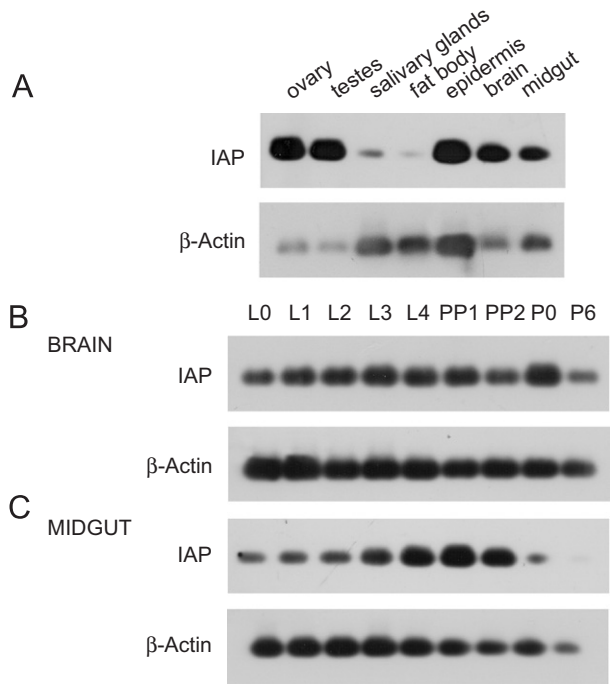

Fig. 3. Expression of *Spodoptera littoralis* IAP (SlIAP) mRNA. (A) Expression in different tissues. Samples were obtained from 4-day-old last instar larvae. (B–C) Expression pattern in the brain (B) and midgut (C) in insects staged on each day of the last larval instar (L0–L6), prepupae (PP1 and PP2) and day 0 and 6 of pupae (P0 and P6). Equal amounts of total RNA were analysed by RT-PCR followed by Southern blotting. In all cases, *S. littoralis* β-actin levels were used as a reference, and the Southern blots shown are representative of three replicates.

One of the first changes in cells undergoing apoptosis is DNA fragmentation, and resulting DNA fragments can be identified using the TUNEL assay, which consists on labelling 3′-OH nucleotide termini, in this case with fluorescent dUTP. In *S. littoralis* midgut, TUNEL positive cells were not detected until the end of the last larval instar, when fluorescence was observed in a few individual cells (Fig. 5A). In prepupal stage, some small patches of labelled cells appeared, but intensity and extension of staining was maximal in freshly formed pupae (P0, Fig. 5G), thus indicating that programmed cell death starts actively at the onset of pupation process. Labelling began to fall down from day 4 of pupal stage (Fig. 5J), and dissapeared three days later (Fig. 5M).

Regions of high lysosomal activity and phagocytosis are also characteristic of cell death processes. Therefore, LysoTracker staining was used to localize these regions in *S. littoralis* midgut. In last larval instar, no detectable staining was observed (Fig. 5B), but prepupae showed incipient LysoTracker positive structures (Fig. 5E). Early pupae midguts displayed strong red staining, which remained intense during the whole pupal stage (Fig. 5(H,K,N). LysoTracker spots can reach relatively big sizes, close to nucleus size (Fig. 5H, inset) due to secondary lysosome fusion. As expected, cells stained with LysoTracker were not marked with nuclear staining TOPRO-3, because the nucleus of these cells had disintegrated. Simultaneous occurrence of dying cells (TOPRO-3 negative and LysoTracker positive) and intact cells (vice versa)

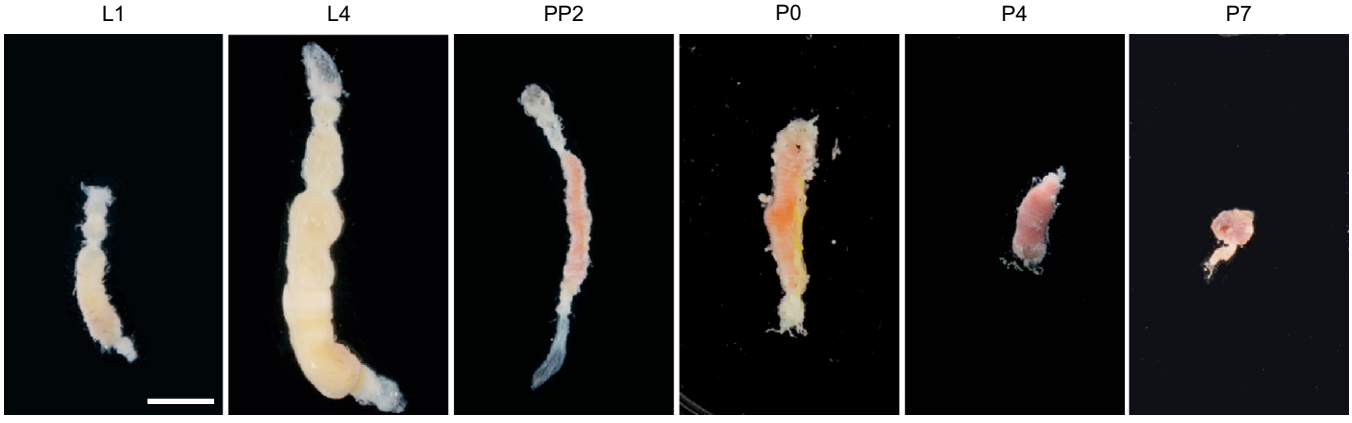

Fig. 4. Midgut morphology of *Spodoptera littoralis*. Stages shown are: 1-day-old last instar larvae (L1), 4-day-old last instar larvae (L4), 2-day-old prepupae (PP2), freshly formed pupae (P0), 4-day-old pupae (P4) and 7-day-old pupae (P7). Scale bar: 5 mm.

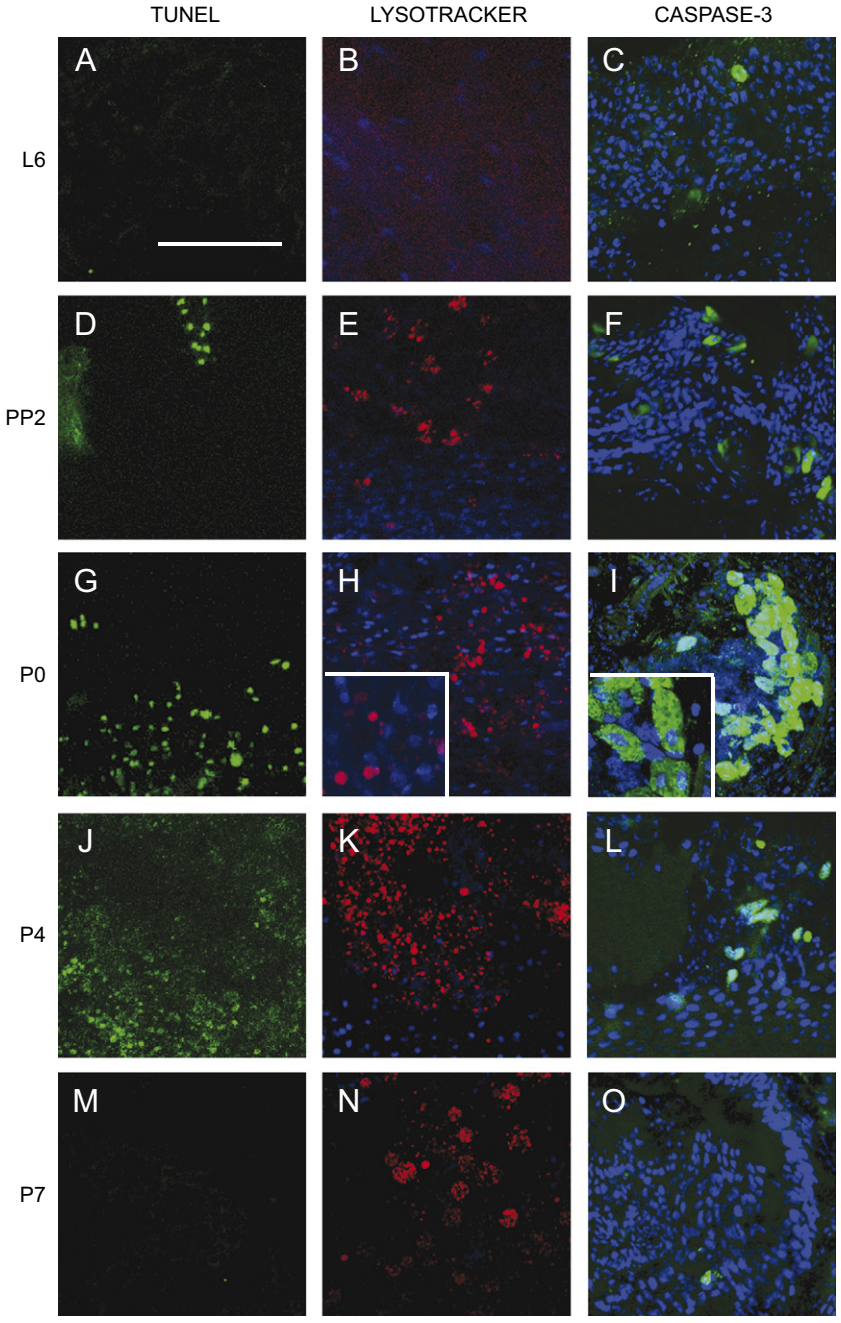

Fig. 5. Cell death in the midgut during larval–pupal metamorphosis of *Spodoptera littoralis*, as shown (columns) by TUNEL labelling, LysoTracker staining and Caspase-3 immunohistochemistry. Stages shown (files) are: 6-day-old last instar larvae (L6), 2-day-old prepupae (PP2), freshly formed pupae (P0), 4-day-old pupae (P4) and 7-day-old pupae (P7). Images show the lumen side of the midgut. Blue spots in columns Lysotracker and Caspase-3 correspond to TOPRO-3 nuclear staining. Scale bar: 100 μm. Insets (in H and I) are 6× magnified with respect to the panels.

indicates that cell death do not proceed synchronically in the whole midgut, but rather trough discrete and successive patches.

Immunohistochemistry using caspase-3 antibody showed the appearance of caspase activity in prepupae midguts (Fig. 5F). The number of labelled cells increased until pupal ecdysis (Fig. 5L), and then decreased until day 7 of the pupal stage, when disappeared (Fig. 5O). As expected, caspase-3 labelling is found in the cytoplasm, and not in the nucleus, which is stained only with TOPRO-3 (Fig. 5I, inset).

4. Discussion

The new lepidopteran IAP from *S. littoralis*, SlIAP, is 382 amino acids long and shows two BIR motifs and one RING finger, which is characteristic of most IAP proteins. A typical animal IAP protein includes between one and

three BIR motifs and one RING finger, whereas baculoviral IAPs contain one or two BIR motifs, and one or none RING finger. With the description of the SlIAP presented herein, *S. littoralis* becomes one of the few cases where the host and the specific viral counterpart IAPs are available. Until now, the described IAPs of *Spodoptera* spp. contain two BIR motifs and the RING finger. On the other hand, baculoviral SlNPV-IAP has been reported as a 15 kDa polypeptide with only one BIR motif, a RING finger and a third specific acidic-rich motif (Liu et al., 2003). SlNPV-IAP is able to delay, but not to suppress, programmed cell death induced by replication of a recombinant AcMNPV deficient in *p*35 (Liu et al., 2003). Sequence alignments and phylogenetic analyses have revealed that the BIR motif of SlNPV-IAP is more similar to BIR1 than to BIR2 motifs of *Spodoptera* spp. From a phylogenetical point of view, IAPs including only one BIR motif and the RING finger, form a cluster separated from that of IAPs containing two BIR domains and one RING finger, due to BIR motif divergence (Liu et al., 2003). Accordingly, SlIAP sequence is more similar to other baculoviral IAPs containing two BIR motifs than to SlNPV-IAP which only contains one.

Our studies have shown that SlIAP is expressed in ovary, testes, salivary gland, fat body, epidermis, brain and midgut tissues of *S. littoralis* last larval instar. Thus, IAP expression seems to be required to prevent premature cell death in these larval tissues. Interestingly, mRNA levels in salivary glands and fat body appeared to be lower in comparison with the other tissues. This may be related with the fact that, during insect metamorphosis, salivary gland undergo rapid and massive cell death (Lee and Baehrecke, 2001; Lee et al., 2002b) and larval fat body dissociates and persists as individual fat cells that are eventually removed by a caspase cascade (Aguila et al., 2007).

Sequential expression studies on midgut and brain tissues revealed that, whereas SlIAP mRNA levels in the brain do not fluctuate significantly, those of the midgut show a particular pattern, with a large peak centred in the prepupal stage. This probably reflects the distinct ways in which cell death process plays on them, given that midgut undergoes a dramatic remodelling during the larval–pupal transition, whereas brain tissues show continuous production and degeneration of neurones throughout larval and pupal stages (Nordlander and Edwards, 1969). In the moth *Heliothis virescens*, expression patterns of caspase-1, ICE and IAP in the midgut during last larval and pupal stages have been reported (Parthasarathy and Palli, 2007). IAP mRNA levels showed a narrow peak on day 2 of last larval instar, then decreased and remained low until day 1 of the pupal stage, where they showed a modest increase. The activation of caspase expression occurred after full IAP down regulation (Parthasarathy and Palli, 2007). The expression of *H. virescens* IAP during the larval–pupal transition differs with respect to that described herein for SlIAP, which suggests that the timing of midgut cell death events or the mechanisms of IAP regulation may be different in the two moths.

Macroscopical examination indicated that midgut morphology changed during metamorphosis from a semi-transparent, cylindrical structure in last instar larvae to a brownish globular mass in pupae. Gross morphological changes, which served us as a frame for more detailed microscopy studies, are similar to those described for other lepidopterans, like *Pieris brassicae* (Komuves et al., 1985) or *Galleria mellonella* (Uwo et al., 2002).

Microscopy studies using TUNEL assays, LysoTracker staining and caspase-3 immunohistochemistry, indicate that *S. littoralis* midgut epithelium death proceeds through discrete and successive patches of dying cells, a feature that has been reported in other insects, such as the fruitfly *D. melanogaster* and a number of lepidopteran species (Komuves et al., 1985; Lee et al., 2002a; Uwo et al., 2002). Autophagy has been shown to be the key mechanism for larval midgut death in a number of insects (Nopanitaya and Misch, 1974; Komuves et al., 1985; Lee et al., 2002a). Dying larval midgut of *S. littoralis*, however, show markers of both authophagy and apoptosis, but data available do not allow to discriminate whether authophagy is required for the death of these tissues or if it is just coincident with apoptosis. In this context, it is worth noting that autophagy and apoptosis share a number of mechanisms and steps, for example, the involvement of effector caspases (Jiang et al., 1997; Lee et al., 2002a; Yin and Thummel, 2004).

The comparison of results from microscopy examination with those from SlIAP expression studies in the midgut, indicates that cell death starts actively at the onset of pupation, coinciding with the dramatical decrease of SlIAP mRNA levels. This coincidence points to an inhibitory role of SlIAP on apoptosis, as expected.

Acknowledgement

Financial support from the Spanish Ministry of Science and Technology (project AGL2005-00773 to X. Bellés) and the Generalitat de Catalunya (2001 SGR 003245) is gratefully acknowledged. Ll. Vilaplana is recipient of a post-doctoral contract from and N. Perera is recipient of a technician contract, both from CSIC under the I3P program.

References

Aguila, J.R., Suszko, J., Gibbs, A.G., Hoshizaki, D.K., 2007. The role of larval fat cells in adult *Drosophila melanogaster*. J. Exp. Biol. 210, 956–963.

Birnbaum, M.J., Clem, R.J., Miller, L.K., 1994. An apoptosis-inhibiting gene from a nuclear polyhedrosis virus encoding a polypeptide with Cys/His sequence motifs. J. Virol. 68, 2521–2528.

Clem, R.J., Duckett, C.S., 1998. The *IAP* genes: unique arbiters of cell death. Trends Biochem. Sci. 23, 159–162.

Clem, R.J., Miller, L.K., 1994. Control of programmed cell death by the baculovirus genes *p*35 and *iap*. Mol. Cell. Biol. 14, 5212–5222.

Chai, J., Yan, N., Huh, J.R., Wu, J.W., Li, W., Hay, B.A., Shi, Y., 2003. Molecular mechanism of Reaper-Grim-Hid-mediated suppression of

DIAP1-dependent Dronc ubiquitination. Nat. Struct. Biol. 10, 892–898.
Crook, N.E., Clem, R.J., Miller, L.K., 1993. An apoptosis-inhibiting baculovirus gene with a zinc finger-like motif. J. Virol. 67, 2168–2174.
Deveraux, Q.L., Takahashi, R., Salvesen, G.S., Reed, J.C., 1997. X-linked IAP is a direct inhibitor of cell-death proteases. Nature 388, 300–304.
Deveraux, Q.L.a.R.J.C., 1998. IAP family proteins: suppressors of apoptosis. Genes Dev 13, 239–252.
Fraser, A., Evan, G., 1996. A license to kill. Cell 85, 781–784.
Freemont, P.S., Hanson, I.M., Trowsdale, J., 1991. A novel cysteine-rich sequence motif. Cell 64, 483–484.
Frohman, M.A., Dush, M.K., Martin, G.R., 1988. Rapid production of full-length cDNAs from rare transcripts: amplification using a single gene-specific oligonucleotide primer. Proc. Natl. Acad. Sci. USA 85, 8998–9002.
Goyal, L., McCall, K., Agapite, J., Hartwieg, E., Steller, H., 2000. Induction of apoptosis by *Drosophila* reaper, hid and grim through inhibition of IAP function. Embo J. 19, 589–597.
Hay, B.A., 2000. Understanding IAP function and regulation: a view from *Drosophila*. Cell Death Differ 7, 1045–1056.
Hay, B.A., Wassarman, D.A., Rubin, G.M., 1995. *Drosophila* homologs of baculovirus inhibitor of apoptosis proteins function to block cell death. Cell 83, 1253–1262.
Hinds, M.G., Norton, R.S., Vaux, D.L., Day, C.L., 1999. Solution structure of a baculoviral inhibitor of apoptosis (IAP) repeat. Nat. Struct. Biol. 6, 648–651.
Huang, Q., Deveraux, Q.L., Maeda, S., Salvesen, G.S., Stennicke, H.R., Hammock, B.D., Reed, J.C., 2000. Evolutionary conservation of apoptosis mechanisms: lepidopteran and baculoviral inhibitor of apoptosis proteins are inhibitors of mammalian caspase-9. Proc. Natl. Acad. Sci. USA 97, 1427–1432.
Huang, Q., Deveraux, Q.L., Maeda, S., Stennicke, H.R., Hammock, B.D., Reed, J.C., 2001. Cloning and characterization of an inhibitor of apoptosis protein (IAP) from *Bombyx mori*. Biochim. Biophys. Acta. 1499, 191–198.
Jiang, C., Baehrecke, E.H., Thummel, C.S., 1997. Steroid regulated programmed cell death during *Drosophila* metamorphosis. Development 124, 4673–4683.
Komuves, L.G., Sass, M., Kovacs, J., 1985. Autophagocytosis in the larval midgut cells of *Pieris brassicae* during metamorphosis. Cell Tissue Res. 240, 215–221.
Kumar, S., Cakouros, D., 2004. Transcriptional control of the core cell-death machinery. Trends Biochem. Sci. 29, 193–199.
Lee, C.Y., Baehrecke, E.H., 2001. Steroid regulation of autophagic programmed cell death during development. Development 128, 1443–1455.
Lee, C.Y., Cooksey, B.A., Baehrecke, E.H., 2002a. Steroid regulation of midgut cell death during *Drosophila* development. Dev. Biol. 250, 101–111.
Lee, C.Y., Simon, C.R., Woodard, C.T., Baehrecke, E.H., 2002b. Genetic mechanism for the stage- and tissue-specific regulation of steroid triggered programmed cell death in *Drosophila*. Dev. Biol. 252, 138–148.
Liao, W.T., Yang, Y., Wu, X.F., 2002. Expression and functional analysis of an inhibitor of apoptosis protein from *Trichoplusia ni*. Biochem. Biophys. Res. Commun. 293, 675–679.
Liston, P., Fong, W.G., Korneluk, R.G., 2003. The inhibitors of apoptosis: there is more to life than Bcl2. Oncogene 22, 8568–8580.
Liu, Q., Chejanovsky, N., 2006. Activation pathways and signal-mediated upregulation of the insect *Spodoptera frugiperda* caspase-1. Apoptosis 11, 487–496.
Liu, Q., Qi, Y., Chejanovsky, N., 2003. Identification and classification of the *Spodoptera littoralis* nucleopolyhedrovirus inhibitor of apoptosis gene. Virus Genes 26, 143–149.
Liu, Q., Qi, Y., Chejanovsky, N., 2005. *Spodoptera littoralis* caspase-1, a Lepidopteran effector caspase inducible by apoptotic signaling. Apoptosis 10, 787–795.
Nopanitaya, W., Misch, D.W., 1974. Developmental cytology of the midgut in the flesh-fly, *Sarcophaga bullata* (Parker). Tissue Cell 6, 487–502.
Nordlander, R.H., Edwards, J.S., 1969. Postembryonic brain development in the monarch butterfly, *Danaus plexippus plexippus, L.* Dev. genes Evol. 162, 197–217.
Parthasarathy, R., Palli, S.R., 2007. Developmental and hormonal regulation of midgut remodeling in a lepidopteran insect, *Heliothis virescens*. Mech. Dev. 124, 23–34.
Poitout, S., Bues, R., 1974. Linolenic acid requirements of lepidoptera Noctuidae Quadrifinae Plusiinae: *Chrysodeixis chalcites* Esp., *Autographa gamma L. Macdunnoughia confusa* Stph., *Trichoplusia ni* Hbn. reared on artificial diets. Ann. Nutr. Aliment 28, 173–187.
Roy, N., Deveraux, Q.L., Takahashi, R., Salvesen, G.S., Reed, J.C., 1997. The c-IAP-1 and c-IAP-2 proteins are direct inhibitors of specific caspases. Embo J 16, 6914–6925.
Salvesen, G.S., Duckett, C.S., 2002. IAP proteins: blocking the road to death's door. Nat. Rev. Mol. Cell Biol. 3, 401–410.
Sun, C., Cai, M., Gunasekera, A.H., Meadows, R.P., Wang, H., Chen, J., Zhang, H., Wu, W., Xu, N., Ng, S.C., Fesik, S.W., 1999. NMR structure and mutagenesis of the inhibitor-of-apoptosis protein XIAP. Nature 401, 818–822.
Uwo, M.F., Ui-Tei, K., Park, P., Takeda, M., 2002. Replacement of midgut epithelium in the greater wax moth, *Galleria mellonella*, during larval-pupal moult. Cell Tissue Res 308, 319–331.
Vaux, D.L., Korsmeyer, S.J., 1999. Cell death in development. Cell 96, 245–254.
Vucic, D., Kaiser, W.J., Harvey, A.J., Miller, L.K., 1997. Inhibition of reaper-induced apoptosis by interaction with inhibitor of apoptosis proteins (IAPs). Proc. Natl. Acad. Sci. USA 94, 10183–10188.
Vucic, D., Kaiser, W.J., Miller, L.K., 1998. Inhibitor of apoptosis proteins physically interact with and block apoptosis induced by *Drosophila* proteins HID and GRIM. Mol. Cell. Biol. 18, 3300–3309.
Wyllie, A.H., Kerr, J.F., Currie, A.R., 1980. Cell death: the significance of apoptosis. Int. Rev. Cytol. 68, 251–306.
Yin, V.P., Thummel, C.S., 2004. A balance between the diap1 death inhibitor and reaper and hid death inducers controls steroid-triggered cell death in *Drosophila*. Proc. Natl. Acad. Sci. USA 101, 8022–8027.
Zachariou, A., Tenev, T., Goyal, L., Agapite, J., Steller, H., Meier, P., 2003. IAP-antagonists exhibit non-redundant modes of action through differential DIAP1 binding. Embo J 22, 6642–6652.
Zhu, J., Miura, K., Chen, L., Raikhel, A.S., 2000. AHR38, a homolog of NGFI-B, inhibits formation of the functional ecdysteroid receptor in the mosquito *Aedes aegypti*. Embo J 19, 253–262.